Boletim da Sociedade Astronômica Brasileira, **37**, no. 1, 167-170

The interplay between stellar and black hole feedbacks in dwarf spheroidal galaxies

J. F. Soares, G. A. Lanfranchi & A. Caproni

[1] Núcleo de Astrofiisica – NAT, Universidade Cidade de São Paulo. e-mail: ppg.afc@unicid.edu.br

Abstract. Local group dwarf spheroidal galaxies are known to have no detectable neutral gas, however the physical mechanism that consumed or removed their gas is still unknown. In this work, the effects of the feedback from supernovae of types Ia and II on the dynamics of the gaseous content of a classical dwarf spheroidal galaxy are investigated by means of a non-cosmological 3D hydrodynamic simulation code. Our results suggest that type Ia supernovae are more effective in expelling the gas out of the galaxy whereas type II supernova remove the gas from the central regions of the system. The spatial distribution of the supernovae is more important to the gas loss than the temporal distribution, but both should be taken into account in stellar feedback studies.

Resumo. Sabe-se que as galáxias esferoidais anãs do Grupo Local não possuem gás neutro detectável, no entanto o mecanismo físico que consumiu ou removeu seu gás ainda é desconhecido. Neste trabalho, os efeitos do feedback de supernovas dos tipos Ia e II sobre a dinâmica do conteúdo gasoso de uma galáxia esferoidal anã clássica são investigados por meio de um código tridimensional de simulação hidrodinâmica não cosmológica. Nossos resultados sugerem que as supernovas do tipo Ia são mais eficazes em expulsar o gás da galáxia, enquanto as supernovas do tipo II removem o gás das regiões centrais do sistema. A distribuição espacial das supernovas é mais importante para a perda de gás do que a distribuição temporal, mas ambas devem ser levadas em consideração em estudos de retroalimentação estelar.

Keywords. Galaxies: dwarf – Galaxies: evolution – Hydrodynamics

1. Introduction

When the classical dwarf spheroidal galaxies (dSph) were first detected (Shapley 1938), they were considered simple systems, very similar to globular clusters, without complex structures, with a single stellar population, and uniform chemical properties. As more detailed observations emerged, the scenario changed drastically. It is now known that these galaxies are characterized by different stellar populations, chemical enrichment not yet fully explained, complex star formation histories, and exhibit a large amount of dark matter (Tolstoy, Hill & Tosi 2009). Completing this scenario, all analyzed dSph share a common feature: the total absence of detectable neutral gas (Grcevich & Putman 2009). How the gas is removed from the galaxy or is consumed internally remains a critical point.

Stellar feedback is the traditional solution invoked to reconcile discrepancies between cosmological simulations and observations of dwarf galaxies (problems such as too-big-to-fail and core-cusp), as the energy from supernovae (SNe) affects evolution, matter distribution, and gas loss. However, the feedback from intermediate-mass/massive black holes (IMBH/MBH) has emerged as a powerful complementary mechanism (Silk 2017).

Observational evidence of Active Galactic Nuclei (AGN) and outflows in dwarf galaxies is becoming increasingly frequent (e.g., Kaviraj et al. 2019, Manzano-King & Canalizo 2020), with estimates of 10-30% AGN occupation in galaxies in the 10^8 – 10^9 $M_\odot$ range. This activity is associated with perturbed gas kinematics, suggesting the AGN's ability to influence dynamics and quench star formation.

In the Local Group, evidence of IMBHs has been detected in dSphs such as Ursa Minor ($\sim 10^4 - 10^5$ $M_\odot$) and Leo I ($\sim 3 \times 10^6$ $M_\odot$). DSphs are notably characterized by the complete absence of neutral gas, although simulations show that stellar feedback from SNe is not sufficient for the total removal of gas.

Thus, the IMBH outflow emerges as a potential internal mechanism, but recent studies (Lanfranchi et al. 2021) indicate that its impact is significantly reduced in a non-homogeneous interstellar medium (ISM), suggesting that a complex interaction between stellar feedback and IMBH feedback is crucial.

The role of an IMBH outflow and the complex interaction between stellar feedback and IMBH feedback were investigated. Specifically, the different roles played by different types of SNe (type II and Ia) in the internal dynamics and gas removal of a typical isolated dSph were analyzed.

2. The Hydrodynamical Code and Initial Setup

Non-cosmological three-dimensional hydrodynamical simulations of the gas of an isolated dSph galaxy were performed to analyze the interaction between the outflow from a central IMBH and stellar feedback and their effects on gas removal from the system, using the PLUTO code [1]. PLUTO (Mignone et al. 2007) is a fluid dynamics code written in C programming language that uses finite elements to integrate the system of differential equations in conservative form.

The initial simulation setup was based on the observational characteristics of the classical dSph Ursa Minor (Caproni et al. 2017, Lanfranchi et al. 2021). Assuming an initial baryonic-to-dark-matter ratio derived from the cosmic microwave background radiation and a cored and static dark matter gravitational potential, the total dark matter halo mass is estimated as $M_h \approx 1.51 \times 10^9$ $M_\odot$ and the initial gas mass is $M_{g0} \sim 2.94 \times 10^8$ $M_\odot$. The interstellar medium is initially in hydrostatic equilibrium with the dark matter potential (McFerlan et al. 1999).

The galactic gas distribution was evolved over 1 Gyr. The galaxy was simulated within a computational cube 3.6 kpc on a side, with 180^3 cells, using Brazilian supercomputers (Sdumont).

[1] http://plutocode.ph.unito.it/

The computational box is divided into three regions with different resolutions, the innermost one being 30 pc/cell.

Stellar feedback and the outflow from a central IMBH are considered in all simulations:

- Stellar Feedback (SNe): The total number of SNe and their temporal distribution are based on chemical evolution models for Ursa Minor (Lanfranchi & Matteucci 2010). An energy of 10^{51} erg is injected per event. The injection location differs by type: for SNe II, the choice of the cell for energy injection is made according to the gas density: the higher the density, the higher the probability of the cell being chosen. If there is more than one cell with high density, the choice among them will be random. SNe Ia have a much longer timescale for occurrence (up to the order of 1 Gyr after star formation) and can therefore explode in locations distant from the high-density region where they formed. Thus, the choice of the cell where the energy of each SN Ia is injected is entirely random.
- IMBH Outflow: A density of 0.01 cm^{-3} and different injection velocities (v_i = 1500 and 2000 km s^{-1}) are inserted into the two central cells of the adopted computational box along one axis of the Cartesian coordinate system. The density and velocity injection values were established within a range corresponding to the observationally estimated mass for the central black hole and to the AGN luminosity values in dwarf galaxies (Maccarone et al. 2005, Lora et al. 2009, Nucita et al. 2013, Manni et al. 2015, Mezcua & Sánchez 2020) and following the results of Lanfranchi et al. (2021).

3. Results

Two main simulations were performed with different IMBH injection velocities: v_i = 1500 km s^{-1} (simulation SV1500TXA) and 2000 km s^{-1} (simulation SV2000TXA).

To analyze the effect of the outflow in a medium perturbed by SNe, the SNe formation rate, according to the chemical evolution model (Lanfranchi & Matteucci 2004, Lanfranchi & Matteucci 2007), was modified. Both simulations utilize the SNe rate multiplied by a factor of 2.

To quantify the gas mass loss from the galaxy, the fraction of remaining mass in different regions is estimated as a function of time, by numerically integrating the obtained gas density distribution.

3.1. Mass fraction

The variation in the fraction of remaining initial gas mass ($M_{\rm gas}$) was analyzed within a spherical volume with the core radius (300 pc) and within the tidal radius (950 pc), comparing simulations SV1500TXA and SV2000TXA.

Within the Core Radius (300 pc): The reduction of $M_{\rm gas}$ is less intense in the first million years for SV1500TXA compared to SV2000TXA, due to the difference in the IMBH injection velocities. Around 50 Myr, the SV2000TXA simulation shows a brief period without gas removal, and a small fraction returns (less than 1%), an effect attributed to Type II SNe explosions, which occur centrally and on a short timescale (> 15 Myr). After ∼ 50 Myr, both simulations expel $M_{\rm gas}$ similarly until the outflow ceases (∼ 250 Myr). Between 300 - 350 Myr, SV2000TXA exhibits a higher mass loss rate (higher derivative), resulting in greater efficiency in expelling $M_{\rm gas}$ until the end of the simulation. At the end of 1 Gyr, SV1500TXA had ∼ 65% of the initial gas mass removed, while SV2000TXA had ∼ 70% removed, the latter being the most efficient scenario within the core radius.

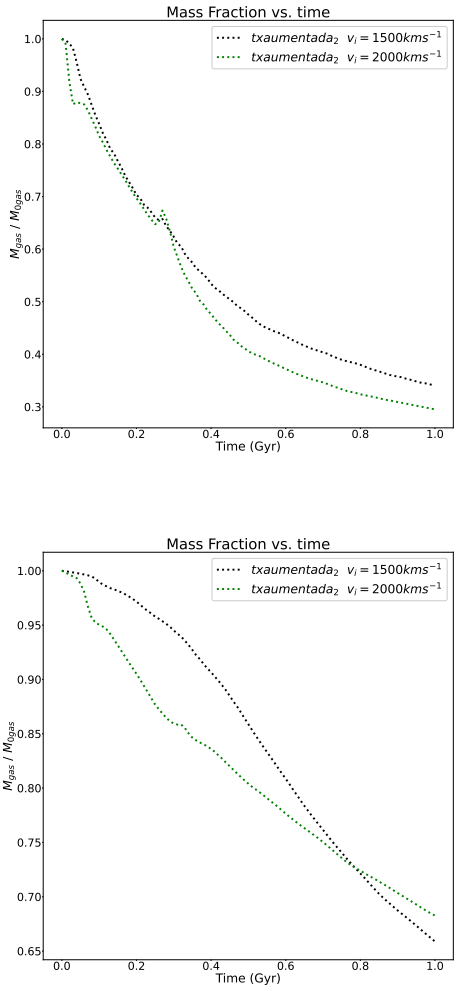

Figure 1. Fraction of initial mass as a function of time within the 300 pc radius (top) and 950 pc radius (bottom) for the simulations: SV1500TXA (dashed black line), SV2000TXA (dashed green line).

Within the 950 pc Radius (Tidal Radius): In the first million years, gas loss differs slightly between the two simulations. From the start until almost 800 Myr, the decrease in $M_{\rm gas}$ is more intense for SV2000TXA (reaching almost 30% removal). After this period, however, SV1500TXA becomes more efficient in removing $M_{\rm gas}$ until the end of the simulation, showing the highest derivative in the graph after the outflow is deactivated. At 1 Gyr, SV1500TXA removed ∼ 35% of the initial gas fraction, while SV2000TXA lost ∼ 30%.

3.1.1. Pressure vs. Radius – v_i = 1500 km s^{-1}

To analyze the gas pressure gradient of the galaxy, plots were generated at different epochs for simulations SV1500TXA and SV2000TXA.

When the IMBH outflow v_i is 1500 km s^{-1}, there is no significant difference until the outflow is deactivated. The pressure remains between 1.10 and 1.20×10^{-10} dyn.cm^{-2} (Figure 2). At 260 Myr, shortly after the outflow is deactivated, the pressure begins to decrease, reaching values of 1×10^{-10} dyn.cm^{-2} at 510 Myr (Figure 4), $8.90 \times$

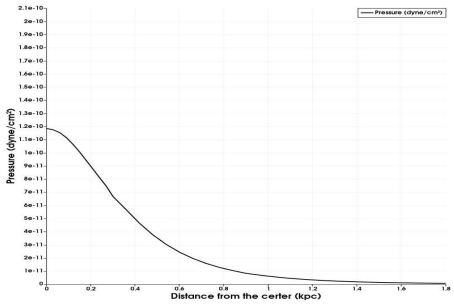

Figure 2. Graph of Gas Pressure (dyne/cm^2) as a function of the galaxy radius at t = 20 Myr for the SV1500TXA simulation.

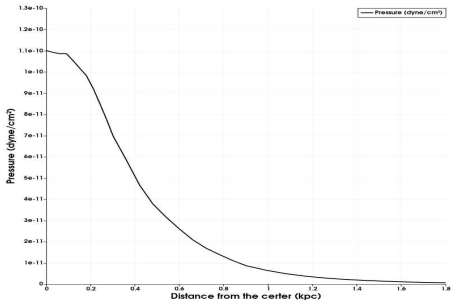

Figure 3. Graph of Gas Pressure (dyne/cm^2) as a function of the galaxy radius at t = 260 Myr for the SV1500TXA simulation.

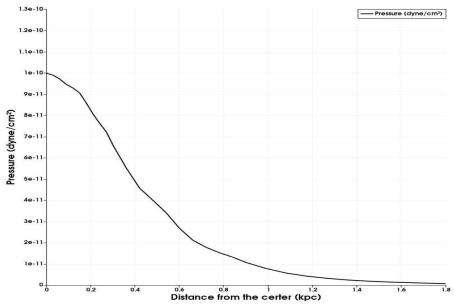

Figure 4. Graph of Gas Pressure (dyne/cm^2) as a function of the galaxy radius at t = 510 Myr for the SV1500TXA simulation.

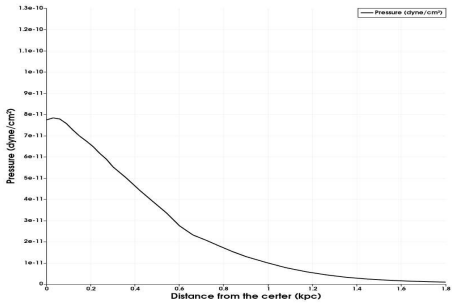

Figure 5. Graph of Gas Pressure (dyne/cm^2) as a function of the galaxy radius at t = 1 Gyr for the SV1500TXA simulation.

10^{-11} dyn.cm^{-2} at 710 Myr and 7.90×10^{-11} dyn.cm^{-2} at the end of the simulation at 1 Gyr (Figure 5).

3.1.2. Pressure vs. Radius – v_i = 2000 km s^{-1}

The gas pressure gradient of the galaxy was also analyzed through five plots, at different epochs, for the SV2000TXA simulation.

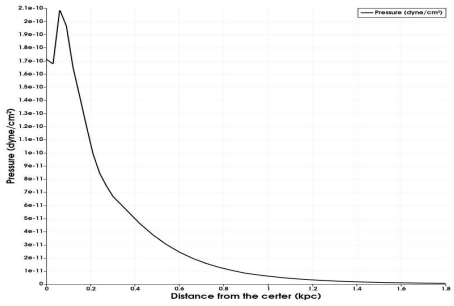

Figure 6. Graph of Gas Pressure (dyne/cm^2) as a function of the galaxy radius at t = 20 Myr for the SV2000TXA simulation.

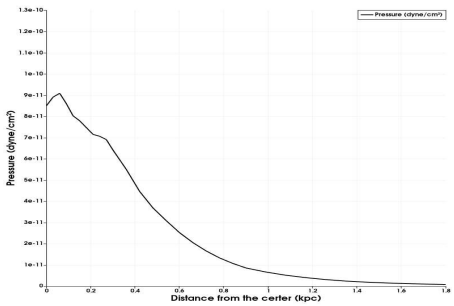

Figure 7. Graph of Gas Pressure (dyne/cm^2) as a function of the galaxy radius at t = 260 Myr for the SV2000TXA simulation.

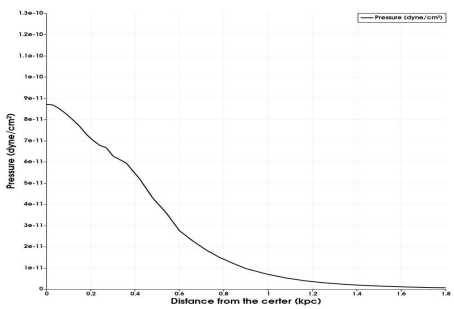

Figure 8. Graph of Gas Pressure (dyne/cm^2) as a function of the galaxy radius at t = 510 Myr for the SV2000TXA simulation.

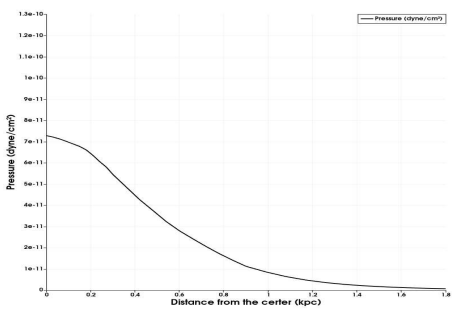

Figure 9. Graph of Gas Pressure (dyne/cm^2) as a function of the galaxy radius at t = 1 Gyr for the SV2000TXA simulation.

In this scenario, with the IMBH outflow v_i at 2000 km s^{-1}, the galaxy gas pressure starts with the same value as the previous case with lower v_i. The values are between 1.10 and 1.20×10^{-10} dyn.cm^{-2}. With a higher v_i, however, there is a peak variation already within the first 20 Myr of the simulation (Figure 6), unlike the previous case where v_i = 1500 km s^{-1} showed no significant difference until the outflow was deactivated. At 20 Myr, the pressure reaches a maximum value of 2.10×10^{-10} dyn.cm^{-2}

in the region 100 pc from the galactic center. Similar to the case with lower v_i, the pressure also decreases after the outflow is deactivated, reaching values of $8.80 - 9 \times 10^{-11}$ dyn.cm^{-2} at 260 Myr (Figure 7), 8.90×10^{-11} dyn.cm^{-2} at 510 Myr (Figure 8), 8×10^{-11} dyn.cm^{-2} at 710 Myr, and 7.20×10^{-11} dyn.cm^{-2} at the end of the simulation at 1 Gyr (Figure 9).

4. Conclusion

In this work, non-cosmological 3D hydrodynamical simulations, adjusted for the dwarf spheroidal galaxy Ursa Minor, were used to investigate the interaction between stellar feedback (SNe II and Ia) and the outflow from a central black hole (IMBH) in scenarios with different injection velocities (v_i = 1500 km s^{-1} and v_i = 2000 km s^{-1}). The evolution of the gas distribution was tracked over 1 Gyr, assuming a static dark matter potential and initial hydrostatic equilibrium.

The analysis of the temporal evolution of the remaining initial gas mass fraction ($M_{\rm gas}$) in two regions — the core radius (300 pc) and the tidal radius (950 pc) — revealed distinct efficiencies:

1. Within the 300 pc radius: SV1500TXA shows an almost linear removal in the first 50 Myr, while SV2000TXA exhibits faster gas loss, followed by a brief mass return (t $\approx$ 50 Myr), possibly due to the influence of the first SNe II explosions. During the period of joint outflow and SNe feedback activity (up to 250 Myr), mass loss is greater for the higher v_i. After the outflow is deactivated and up to 1 Gyr, SV2000TXA remains more efficient, ending with $\sim$ 70% of the initial gas mass removed, compared to $\sim$ 65% for SV1500TXA.
2. Within the 950 pc radius: In this volume, the SV2000TXA simulation is more efficient in removing $M_{\rm gas}$ up to $\sim$ 800 Myr. However, after the outflow ceases, the situation reverses: SV1500TXA (lower v_i) demonstrates greater efficiency in removing gas beyond the tidal radius, showing the highest mass loss rate (derivative) until the end of the simulation. At 1 Gyr, the remaining $M_{\rm gas}$ is $\sim$ 66% in SV1500TXA (a removal of 34%) and $\sim$ 68% in SV2000TXA (a removal of 32%).

The analysis of the pressure gradient corroborates the complexity of the interaction: while the outflow is active, scenarios with higher v_i (SV2000TXA) result in higher pressure. However, after the outflow is deactivated, the pressure gradient is consistently higher in the lower v_i scenario (SV1500TXA). These results indicate that the interaction between the IMBH outflow and SNe feedback is fundamental and cannot be analyzed separately, being crucial for understanding gas mass loss in dwarf spheroidal galaxies, contrary to models that only compare total power or local escape velocities.

References

Caproni, A., Lanfranchi, G. A., Baio, G. H. C., Kowal, G., Falceta-Gonçalves, D., 2017, The Astrophysical Journal, 838.

Lanfranchi, G. A., & Matteucci, F., 2004, Monthly Notices of the Royal Astronomical Society, 345, 1338.

Lanfranchi, G. A., & Matteucci, F., 2007, Astronomy & Astrophysics, 468, 927.

Lanfranchi, G. A., & Matteucci, F., 2010, A&A, 512, A85.

Lanfranchi, G. A., Hazenfratz R., Caproni A., Silk J., 2021, The Astrophysical Journal, 914, 32.

Lora, V., Sanchez-Salcedo, F., J., Raga, A., Esquivel, A., 2009, The Astrophysical Journal, 699, 113.

Maccarone, T.J., Fender, R.P. & Tzioumis, A.K., 2005, Astrophysics and Space Science, 300, 239.

Manni, L., Nucita, A. A., De Paolis, F., Testa, V., Ingrosso, G. A., 2015, Monthly Notices of the Royal Astronomical Society, 451, 2735.

Mezcua, M., and Sánchez,H. D., 2020, The Astrophysical Journal Letters, 898, 2.

Mignone, A., Bodo, G., Massaglia, S., et al., 2007, The Astrophysical Journal, 170, 228.

Nucita, A. A., De Paolis, F., Manni, L., Ingrosso, G., 2013, Nature, 23, 107.

Shapley, H.. 1938, "Two Stellar Systems of a New Kind". Nature, 142, 715

Tolstoy, E., Hill, V., & Tosi, M., 2009, Annual Review of Astronomy and Astrophysics, 47, 371.

Wilson, A. G.. 1955, PASP, 67, 27